Journal of Water Sciences Research,
ISSN: 2251-7405 eISSN: 2251-7413
Vol.7, No.2 , Winter 2015, 39-51, JWSR

JWSR

Assessment of Turbulent Models in Computation of Strongly Curved Open Channel Flows

Omid Seyedashraf[1], Ali Akbar Akhtari[2]*

[1]M.Sc. Hydraulics Engineering., Faculty Member, Department of Civil Engineering, Kermanshah University of Technology, Kermanshah, Iran

[2] Assistant Professor, Hydraulics Engineering Faculty Member, Department of Civil Engineering, Razi University, Kermanshah, Iran

Received: 18 April 2014 Accepted: 14 January 2015

ABSTRACT

Several rigorous turbulent models have been developed in the past years and it can be seen that more research is needed to reach a better understanding of their generality and precision by verifying their applications for distinct hydraulic phenomena; under certain assumptions. This survey evaluates the performance of Standard k-ε, Realizable k-ε, RNG k-ε, k-ω and RSM models in predicting flow behavior in a strongly curved open channel bend. Accordingly, three-dimensional numerical simulations were carried out using a state-of-the-art computational fluid dynamics code, ANSYS-Fluent14, which employs finite volume method to solve the respective governing equations. The models' accuracy were analyzed and compared with observed data from experimental studies on a 90° open channel bend. The results indicate that although the RSM model can precisely capture all the flow characteristics in a strongly curved open channel flow, the Standard k-ε model may be considered as slightly less accurate yet much faster model.

Keywords

Open Channel Bend, Strongly Curved Flow, Turbulent Models, Two-Phase Flow, Volume Of Fluid

Introduction

One of the most distinguishing characteristics of a strongly curved open channel flow is its secondary currents (cross-stream circulation cells), and therefore, the formation of a helical motion along its path that would be inevitable.

This secondary flow is the primary cause of fluctuations in flow velocity, boundary shear stress distribution, intensity and direction of the sediment transport, and overall river morphology. The physical description of the current has been celebrated as the disequilibrium in pressure gradient and force changes at arbitrary sections. These changes gradually reshape the bank form, and affect the amount of bed erosion and sediment transport in river meanders, which is naturally dependent on the river section shape and their morphodynamics (Blanckaert and de Vriend 2003).

In straight channels, turbulence is a determinant factor in formation of flow behaviors, and is the main reason for turbulence driven secondary motions (Rodi and Research 1993). Moreover, the development of helical motion in a curved

Corresponding Author: Akhtari@razi.ac.ir

open channel flow is not much dependent on turbulence, but on the centrifugal forces, and can be numerically simulated with a zero equation turbulence closure (Jia and Wang 1992). However, in practical interests of fluid flow, due to high Reynolds numbers and disturbances caused by irregular boundaries, water currents in rivers or man-made open channels are almost always turbulent (Jackson 1995). Consequently, it is a must to employ a turbulent model in order to obtain accurate simulations in curved open channel flows. On the other hand, the velocity fluctuations and distribution of boundary shear stress induced by the turbulent transfer of mass and momentum can considerably contribute to flow behaviors. For example, in open channel flows and especially in meanders, the factor of flow separation, spreading and mixing of heat and dissolved matters, pollutant, oxygen and amount of sediment transport are closely related to flow turbulence.

The structure of turbulence in a curved open channel flow is different from that of a straight flow, most particularly in a reduction of the turbulent movements toward the outer bank of the bend. Both the outer-bank cell and reduced turbulent activity have a protecting result on the outer bank and the near bottom; therefore, affect the stability of bend and river morphology (Blanckaert and Graf 2001).

Laboratory investigation of flow pattern within open channel bends has fascinated water scientists and engineers for the past seven decades. Revolutionary study of the flow structure in open channel bends is commonly credited to Thompson (1876) who observed the spiral characteristic of flow in a channel bend by injection of dye into the flow. From the time until today, many investigations have been carried out on flows in bends. These studies have become good sources for validation of novel numerical methods. To allude to but a few: Rozovskii (1957) conducted a series of experimental researches on a 180° bend of rectangular cross section with straight inlet and outlet reaches. He measured velocity profiles near the walls and showed that the maximum value of the depth-averaged axial velocity first moves to the inner bank and then to the outer bank right beneath the water surface. The obtained data of his remarkable investigations have been used many times to validate new numerical methods (Leschziner 1979). Ippen and Drinker (1962) examined and defined the distributions, and the values of boundary shear stresses in subcritical flow regimes of the curved reaches of smooth trapezoidal open channels. That was carried out under conditions of subcritical flow. They found that the locations of the maximum shear stresses were commonly found associated with the path of highest velocity. Engelund (1974) illustrated the theory of helical flow in circular bends. The theory was established for steady fully developed uniform flows and for wide rectangular channels. Later, they extended the theory and applied to more complex problems of flow in an open channel bend with movable bed. Blanckaert and de Vriend (2005) carried out several experimental studies of turbulent characteristics in sharp open channel bends. They measured velocity currents with an acoustic Doppler velocity profiler (ADVP) on a fine grid, and derived the mean velocity vector as well as the oscillating velocity vectors. They have also obtained all six turbulent stress components, all higher-order turbulent velocity correlations, and distribution of other attributes of the respective flow. As a more recent experimental investigation, Akhtari (2009 and 2010) carried out several studies on 30°, 60° and 90° strongly curved open channel bends with central radiuses of 60(cm) and a 1.5 ratio of curvature radius to channel width for five

different discharge values. He has gathered extensive data like velocity and water depth profiles, and found that in a distance equal to channel width from the bend entry and bend exit, water surface was not being affected by the curvature.

Besides laboratory studies, recently a large number of numerical investigations have been conducted on flow patterns in strongly curved bends. However, although it is needed to be known how well the different models can handle the numerous complexities present in such case studies, most of them only concentrated on the flow patterns and often did not cover the turbulent nature of the flow. Moreover, the grids used to discretize the computational domain were rather coarse and inaccurate. The following researchers have contributed to the implementation of the numerical methods to predict flow behavior in open channel bends. Kuipers and Vreugdenhil (1973) developed a model to deal with axial current features. Since the model was based on a depth-averaged procedure, it could not simulate secondary flows and therefore, the velocity distribution along bend was not correctly simulated. De Vriend (1976) also applied a three-dimensional mathematical model to simulate the flow features in a similar benchmark. Harrington et al. (1978) utilized a depth-averaged model, without incorporating the essential extra terms to calculate secondary currents and to predict the flow path in a 180° channel bend. However, the results were underestimated due to lack of the secondary motions (Jin and Steffler 1993). Moreover, Lu et al. (1989) showed that the one-dimensional equations of motion in conjunction with theories, which connect the strength of the secondary flow components to flow depths, of channel planform curvature, and depth-averaged mean velocities can be also used to numerically predict the flow characteristics of meandering rivers. Molls and Chaudhry (1995) developed a two-dimensional numerical model to solve unsteady, depth-averaged equations. The equations were obtained by depth-averaging the Navier-Stokes equations from the channel bottom to the water surface. In this investigation, a constant eddy-viscosity turbulent model was employed to estimate Reynolds stresses. The mode1 was validated by experimental data of flow in a 280° open channel bend. Ghamri (1999) developed a two-dimensional vertically averaged governing equation to account for respective problems and employed an implicit Petrov-Galerkin finite element scheme to solve them.

Dealing with turbulence modes, the standard k-ε model is the most commonly used two-equation model (Pope 2000). The model was developed by Launder and Spalding, and the word 'standard' was coined by Jones and Launder, who first presented it in 1972 (Jones and Launder 1972).

Subsequently, many researchers have employed the model numerically simulate open channel flows, to allude to but a few: Leschziner and Rodi (1979) applied it in numerical simulation of a strongly curved open channel flow calculation while the flow was considered fully developed. To map a physical domain with free surface, Ye and McCorquodale (1998) developed a three-dimensional numerical model using k-ε model in conjunction with σ-transformation. The model could handle an unprescribed free surface and nonrectangular, non-prismatic practical channel geometries. Moreover, it was tested by applying it to two typical curved open channel flows, which were a single 270° bend with a sloped outer bank, and a meandering channel with pollutant transport. Hsieh and Yang (2003) assessed efficiency of two-dimensional models for bend flow simulation making use of both a conventional model and a bend-flow model.

Analysis of the numerical data indicated that the maximum relative difference in longitudinal velocity is primarily linked to the relative strength of the secondary flow and the relative length of the channel.

Using a three-dimensional finite volume morphodynamic model, Khosronejad et al. (2007) numerically simulated the channel bed evolution in an S-shaped channel, a 90° and a 135° channel bend. The utilized model was able to solve the Reynolds Averaged Navier-Stokes (RANS) equations, and employed both k-ω and k-ε models to close turbulence. They acquired the sediment concentration distribution and calculated the channel bed evolution using the convection-diffusion and the sediment continuity equations, respectively. Khosronejad (2010) also applied the k-ε model to numerically simulate Dez dam reservoir flow field, and found the maximum values of velocity currents and intensity distribution of flow turbulence.

The current investigation evaluates the performance of five turbulent models for simulation of flow in a strongly curved open channel bend. To illustrate the effectiveness of the models, the experimental data from a laboratory flume with bend were used to verify them (Akhtari 2010). Consequently, the experimental data are compared to the numerical results, and the most accurate models are introduced.

2. Flow Simulation

2.1. Governing Equations

Here, the governing equations used to simulate the flow region are based on conservation of mass and momentum, which are RANS equations. They can be written in their conservative forms and in generalized Cartesian coordinates (x,y,z) as:

$$\frac{\partial(\rho)}{\partial t}+\frac{\partial(\rho u_i)}{\partial x_i}=S_m \qquad (1)$$

$$\frac{\partial(\rho u_i)}{\partial t}+\frac{\partial(\rho u_i u_j)}{\partial x_j}=-\frac{\partial p}{\partial x_i}+\frac{\partial}{\partial x_j}\mu\left[\frac{\partial u_i}{\partial x_j}+\frac{\partial u_j}{\partial x_i}\right]+\frac{\partial\left(-\rho\overline{u_i' u_j'}\right)}{\partial x_j} \qquad (2)$$

where t is time, u_i is the i-th component of the Reynolds-averaged-velocity, x_i the i-th axis with the vertical x_3 axis, ρ is the water density, p is the Reynolds averaged pressure, g is the acceleration due to the gravity, μ is viscosity _which is equal to zero in this study_, and S_m is the mass exchange between two phases (water and air). The term ($-\rho\overline{u_i' u_j'}$) is called Reynolds-stress and has to be modelled in order to close the momentum equation. To do this, the Boussinesq hypothesis has been utilized, which makes a connection between Reynolds-Stresses and the mean rate of deformation:

$$-\rho\overline{u_i' u_j'}=\mu_t\left(\frac{\partial u_i}{\partial x_j}+\frac{\partial u_j}{\partial x_i}\right) \qquad (3)$$

here μ_t is the turbulent viscosity.

The computational domain was divided into a large number of control volumes, and a state-of-the-art CFD code _ANSYS FLUENT 14_ was used to discretize the governing equations and conduct the numerical computations. This code employs the Finite Volume Method (FVM), which involves discretization and integrations of equations over control volumes. It should be noted that, since the unsteady solver will be used to get the velocities and other solution variables, they mentioned parameters now represent time-averaged values instead of instantaneous values.

2.2. Turbulent Models

Five multiple-equation turbulent models were considered and used in conjunction with the non-equilibrium wall-function treatment to carry out the simulations. Standard k-ε model, Realizable k-ε model, Renormalization Group

(RNG) k-ε, k-ω, and the Reynolds Stress Model (RSM) are the turbulent models that were used and included in the equation system in the present study. Accordingly, certain numerical provisions were taken into account for each simulation, like adopting the suitable wall functions incorporating the boundary layer effects close to walls.

The Standard k-ε model is based on transport equations for the turbulence kinetic energy (k) and its dissipation rate (ε). The equation for k contains extra turbulent fluctuation terms, which are unknown. Again using the Boussinesq assumption, these fluctuation terms can be related to the mean flow.

Simplified model equation for k and ε:

$$\frac{\partial(\rho k)}{\partial t} + div(\rho k\mathbf{U}) = div\left[\frac{\mu_t}{\sigma_k} grad\ k\right] + 2\mu_t E_{ij}.E_{ij} - \rho\varepsilon \quad (4)$$

$$\frac{\partial(\rho\varepsilon)}{\partial t} + div(\rho\varepsilon\mathbf{U}) = div\left[\frac{\mu_t}{\sigma_\varepsilon} grad\ \varepsilon\right] + C_{1\varepsilon}\frac{\varepsilon}{k}2\mu_t E_{ij}.E_{ij} - C_{2\varepsilon}\rho\frac{\varepsilon^2}{k} \quad (5)$$

where U is the velocity vector, E_{ij} is the mean rate of deformation tensor, $C_{1\varepsilon}$ and $C_{2\varepsilon}$ are constants, and typically values of 1.44 and 1.92 are used. The Prandtl number σ_k, connects the diffusivity of k to the eddy viscosity and normally a value of 1.0 is used, while the Prandtl number σ_ε connects the diffusivity of ε to the eddy viscosity and generally, a value of 1.30 is used.

The RNG k-ε equations are derived by performing a series of mathematical operations on the instantaneous Navier-Stokes equations. It is similar in form to the Standard k-ε equations but with an additional term in the ε equation for dealings between turbulence dissipation and mean shear. Its appropriate impact of swirl on turbulent currents makes the method applicable to simulate rather swirling flows. For a steady incompressible flow and disregarding the body forces, the turbulent kinetic energy and dissipation rate can be calculated as follows:

$$\rho U_i\frac{\partial k}{\partial x_i} = \mu_t S^2 + \frac{\partial}{\partial x_i}\left(\alpha_k\mu_{\text{eff}}\frac{\partial k}{\partial x_i}\right) - \rho\varepsilon \quad (6)$$

$$\rho U_i\frac{\partial \varepsilon}{\partial x_i} = C_{1\varepsilon}\left(\frac{\varepsilon}{k}\right)\mu_t S^2 + \frac{\partial}{\partial x_i}\left(\alpha_\varepsilon\mu_{\text{eff}}\frac{\partial \varepsilon}{\partial x_i}\right) - C_{2\varepsilon}\rho\left(\frac{\varepsilon^2}{k}\right) - R \quad (7)$$

where R is an extra term related to mean strain and turbulence magnitudes, which is the major difference between the RNG and Standard k-ε model. S could be calculated from the velocity gradients, and α_ε, α_k, $C_{1\varepsilon}$ and $C_{2\varepsilon}$ are derived through RNG theory (Gaudio, Malizia et al. 2011).

Realizable k-ε is another enhanced turbulence model, which shares the identical kinetic energy equation as Standard k-ε model with an enhanced formulation for dissipation rate. Its 'Realizability' stems from the modifications that permit certain mathematical operations followed, which ultimately improve the performance of the model. Similar to the RNG model yet probably more precise and easier to converge. Improved performance for flows involving planar and round jets, boundary layers under strong adverse pressure gradients or separation, rotation, recirculation and strong streamline curvature is the important characteristics of this model.

Its simplified equation is as follows:

$$\rho\frac{D\varepsilon}{Dt} = \frac{\partial}{\partial x_j}\left[\left(\mu + \frac{\mu_t}{\sigma_\varepsilon}\right)\frac{\partial\varepsilon}{\partial x_j}\right] + \rho c_1 S\varepsilon - \rho c_2\frac{\varepsilon^2}{k+\sqrt{\nu\varepsilon}} + c_{1\varepsilon}\frac{\varepsilon}{k}c_{3\varepsilon}G_b \quad (8)$$

where, G_b is the generation of turbulence kinetic energy due to buoyancy.

The k-ω is another two equation turbulence model, which offers largely the same benefits as RNG. In this model, ω is an inverse time

scale that is associated with the turbulence. The model incorporates two partial differential equations. One is the modified version of the equation related to kinetic energy used in the k-ε model in addition to a transport equation for ω. Its numerical behavior is identical to that of the k-ε models and suffers from some of the same difficulties, such as the assumption that μ_t is assumed isotropic.

The turbulent viscosity is calculated as follows:

$$\mu_t = \rho \frac{k}{\omega} \tag{9}$$

RSM closes the RANS equations by solving extra transport equations for six independent Reynolds stresses. Its transport equations resulting from Reynolds averaging are the consequences of the momentum equations with a fluctuating characteristic and one equation for turbulent dissipation. Here, the isotropic eddy viscosity assumption is avoided, and the equations comprise terms that need to be modelled. The model is suitable for precisely predicting complex flows like streamline curvature, swirl, rotation and high strain rate flows, and is recommended to model open channel flow problems (Lu, Hong et al. 2003).

The exact equation for the transport of the Reynolds-stress R_{ij} is as follows.

$$\frac{DR_{ij}}{Dt} = P_{ij} + D_{ij} - \varepsilon_{ij} + \Pi_{ij} + \Omega_{ij} \tag{10}$$

where P_{ij} is the rate of production, D_{ij} is the transport by diffusion, ε_{ij} is the rate of dissipation, $\prod_{ij}$ is the transport due to turbulent pressure-strain interactions and Ω_{ij} is the transport due to rotation.

This equation defines six partial differential equations; as one for the transport of each of the six independent Reynolds stresses. It should be noted that in the case, there was no possibility to determine Reynolds stress parameters explicitly; it is more convenient to use the turbulent kinetic energy parameters instead.

2.3. Model Geometry and Grid Form

The flow region was divided into a number of non-overlapping cells with total 386,400 segments and 409,683 nodes. Out of different possible grid forms, the chosen one is appropriate for both accuracy and minimizing the characteristic time of convergence, which is made of Hexahedron type cells. To attain sound data of the separation tendency in flow, the secondary currents and flow depths, the curved section of the channel was discretized to diminutive elements. Consequently, 175 longitudinal, 50 latitudinal and 28 altitudinal segments were produced in the specified computational domain.

To simulate the fully developed flow, as of the experimental channel, the same length was considered just before the bend.

As depicted in Fig. 1 the flume has a square section with 403 mm× 403 mm dimensions while the radius of curvature is 0.6m, depth of flow 0.12m and the mean velocity in the entrance of the flume is 0.394 m/s.

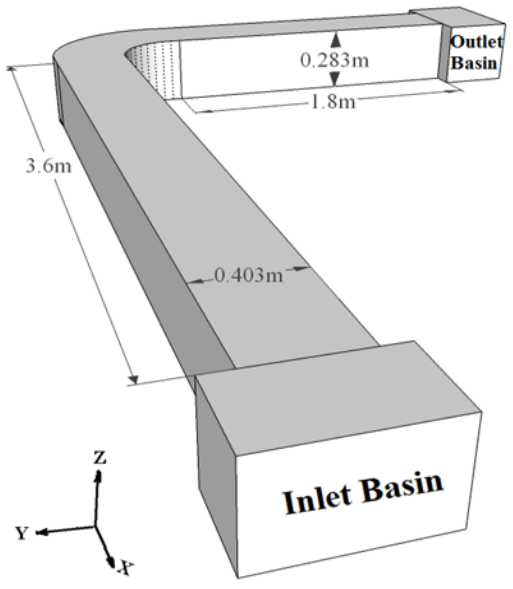

Fig. 1. Schematic layout of the flume with a 90° bend

Fig. 2 shows the applied grid form of the open channel bend in the respective computational domain.

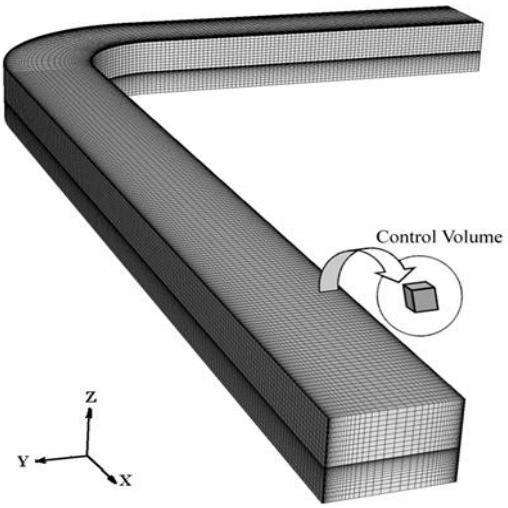

Fig. 2. Grid form of model test

2.3. Numerical Scheme

Equations (1) and (2) are a set of convection equations with velocity and pressure couplings based on control volume method. A general-purpose CFD code was used to conduct the numerical computations presented in this research. The code employs FVM in conjunction with a coupling method, which simultaneously solves the equations in the whole domain through a false time-step algorithm.

Here, the convection terms are discretized using the third-order Monotone Upstream Centered Scheme for Conservation Law (MUSCL). The momentum equations are discretized using the Quadratic Upstream Interpolation for Convective Kinetics (QUICK) scheme (Leonard 1979). The linearized system of equations is preconditioned in order to decrease the eigen-values to the same order of magnitude. Since the flow is incompressible, a pressure-based solver is used to solve the governing equations. The Pressure-Implicit with Splitting of Operators (PISO) method by Issa (1986) is employed to deal with velocity and pressure couplings. This technique incorporates the pressure effect through momentum into continuity in order to obtain correction equations.

The Volume of Fluid (VOF), a free surface tracking technique by Hirt and Nicholas (1981), is utilized to track the free surface and predict the air-water interactions. Its formulation relies on the fact that two or more phases are not interpenetrating and like other advection algorithms must be solved separately. Using this method, for each extra phase added to the system, a variable must be defined in the volume fraction of the phase for computational cells. Moreover, in each cell, the volume fractions of all phases sum to unity.

The special grid form employed to discretize the computational domain, has considerably improved the convergence process. Using the mentioned scheme, about 3500 iterations were accomplished for each simulation in order to reach a full convergence in the computations.

3. Calibration and Validations

The test sections are located at 0°, 45°, and 90° upstream into the bend, and 40 cm and 80 cm after the bend.

Fig. 3 illustrates the comparison of the measured and simulated super-elevation values obtained by five different turbulent models.

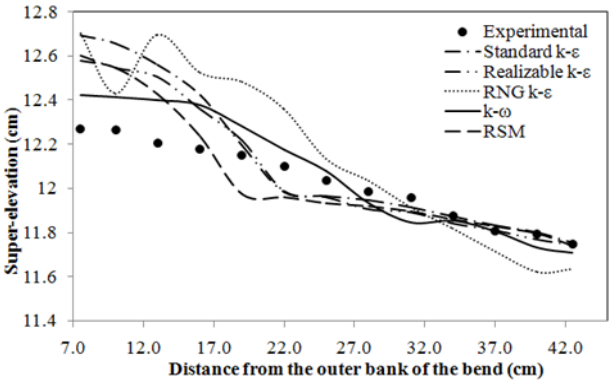

a. 0 degree of the bend

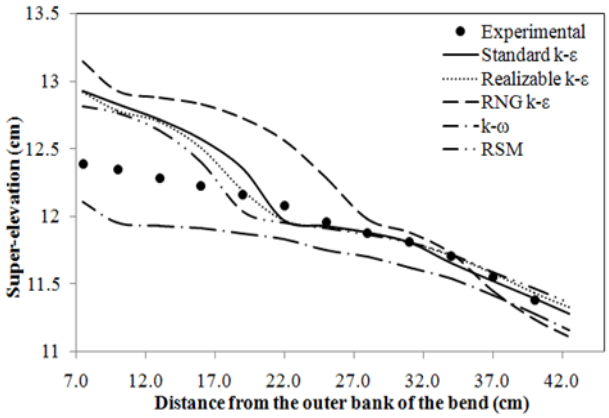

b. 45 degree of the bend

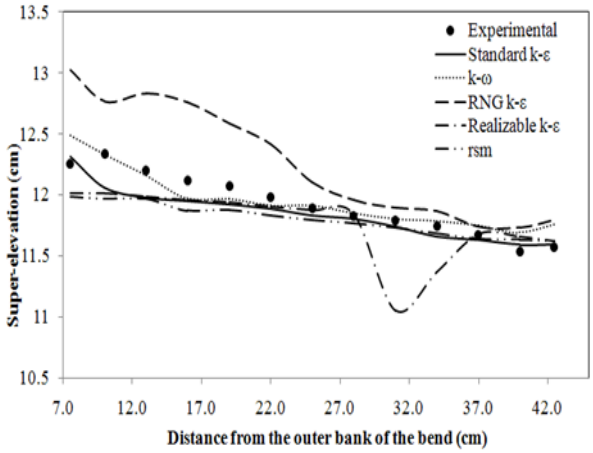

c. 90 degree of the bend

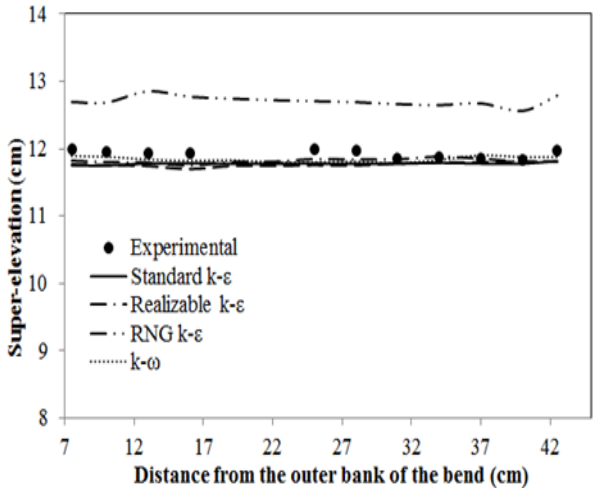

d. 40 centimeters after the bend

Fig. 3. Analogy of the super-elevation values obtained by various turbulent models

The experimental and the numerically predicted flow velocities; using five different turbulent models, are depicted in Fig. 4.

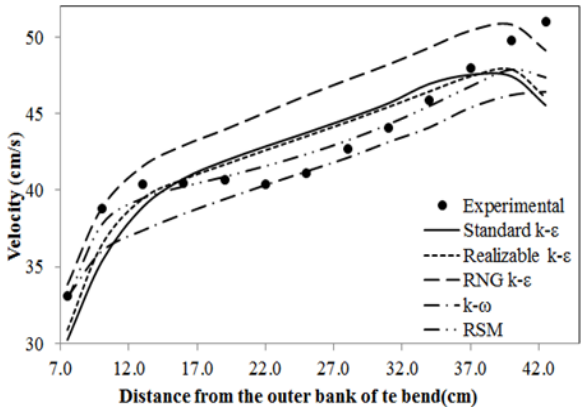

a. 45 degree of the bend

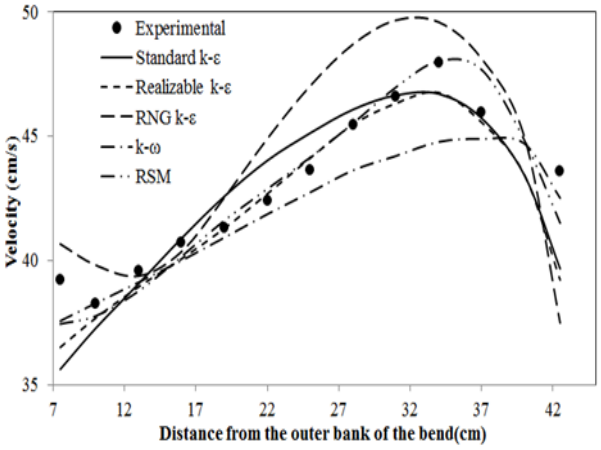

b. 90 degree of the bend

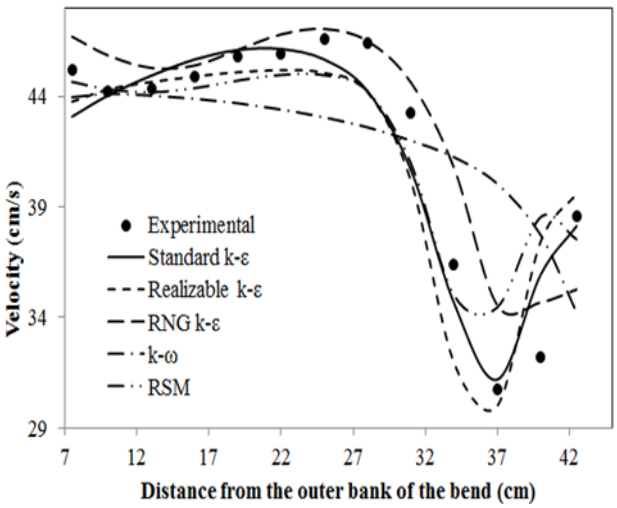

c. 40 centimeters after the bend

Fig. 4. Analogy of velocity values obtained by various turbulent models

Here, the velocities were measured from the middle layers of the flow.

As shown above, all the complex characteristics of flow, like velocities are

predicted reasonably accurate. Moreover, the model demonstrates the secondary flows and the tendency to separation. However, it must be noted that it is not only for the turbulent models themselves, since they are inadequate and flow development in strongly curved open channel bends are significantly affected by pressure forces (Rodi and Research 1993).

To evaluate the accuracy of the adopted scheme, the Root Mean Square Errors (RMSE) of the numerical velocity results are calculated. RMSE is a standard error measure of the values predicted by a model, and is defined as:

$$RMSE\% = \sqrt{\frac{1}{N}\sum_{i=1}^{N}\left(\frac{u_i - u_{Exact}}{u_{Exact}}\right)^2} \times 100 \qquad (11)$$

where, u_i is the numerically obtained velocity value at each node (i), and u_{Exact} is the measured velocity value of the respective node.

The RMSEs of for super-elevation and velocity results are calculated and listed in Tables 1 and 2, respectively.

Table 1.
Root mean square errors for each turbulence model (Super-elevation)

Sections	Standard k-ε	Realizable k-ε	RNG k-ε	k-ω	RSM
0^o	1.67	1.3	2.1	0.93	1.2
45^o	2.10	1.92	3.46	2.10	1.67
90°	1.06	2.30	3.39	0.94	1.49
40*cm*	1.33	0.97	6.54	0.90	1.47
80*cm*	1.72	1.95	2.60	1.59	2.04
Overall	**1.58**	**1.69**	**3.62**	**1.29**	**1.57**

Table 2.
Root mean square errors for each turbulence model (Velocity)

Sections	Standard k-ε	Realizable k-ε	RNG k-ε	k-ω	RSM
0^o	5.80	4.80	7.30	5.00	2.80
45^o	6.56	6.05	5.36	6.87	5.59
90°	9.45	9.25	11.45	10.08	9.96
40*cm*	4.40	6.30	6.10	9.94	7.00
80*cm*	5.60	6.10	9.30	7.04	4.80
Overall	**6.36**	**6.50**	**7.90**	**7.79**	**6.03**

From Table 1, it can be seen that the k-ω turbulence model has captured the free surface reasonably accurate. Moreover, from Table 2, it can be inferred that the RSM turbulence model following with the Standard k-ε model trends toward accurate predictions.

Using the RSM model, the main difficulty is that this model is very costly and more CPU time is required to solve its extra equations. Accordingly, in this research, the Standard k-ε model is introduced as the preferred turbulence model because of its lower computational costs.

Fig. 5 depicts the distribution of the mean tangential velocities at five cross sections and compares the experimentally and numerically obtained data along the bend.

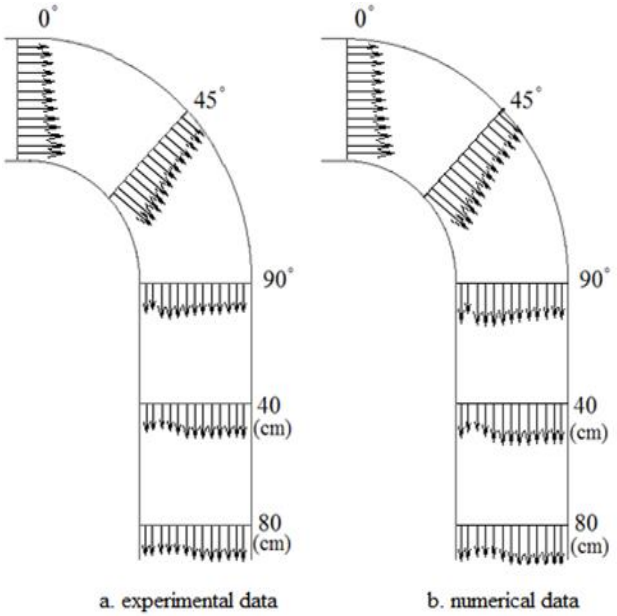

Figure 5: Distribution of mean velocities along the channel bend, obtained by experimental and numerical investigations)

Here, the Standard k-ε turbulent model is employed to conduct the numerical simulation.

Fig. 6 demonstrates the growth process of transverse circulation of water, also known as helical motion, through and after the bend. The portrayed vectors are the measured quantities of transverse velocity vector fields.

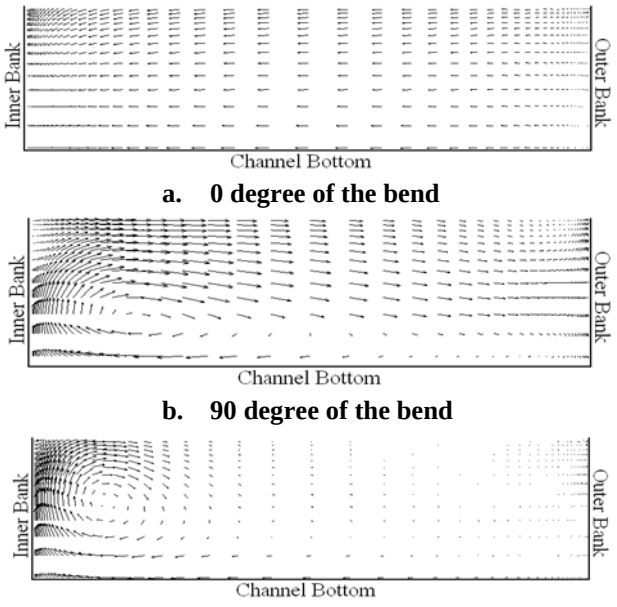

a. 0 degree of the bend

b. 90 degree of the bend

c. 60 centimeters after the bend

Fig. 6. Evolution of secondary currents along the open channel bends at different sections

As it can be seen in this figure, the secondary flow has a center of rotation, which gently shifts inwards in its path through the bend.

4. Conclusions

The objective of this study is to compare the performances of five multi-equation turbulent models in predicting flow characteristics in strongly curved open channel curves. In such cases, two-dimensional models are inadequate to characterize the flow conditions due to existence of secondary currents and therefore, the helical nature of the flow. Consequently, three-dimensional models are highly beneficial.

Numerical simulations were carried out for an open channel flow at a strongly curved bend using a state-of-the-art CFD code, which employs the FVM method to approximately solve the governing equations. Accordingly, the VOF free-surface flow model was incorporated with five multi-equation turbulent models namely Standard k-ε, Realizable k-ε, RNG k-ε, k-ω and RSM. The available experimental measurements were set as a criterion for comparison of the employed models and assess their precision. Since the model results are sensitive to the grid form, required care was taken into account while meshing the computational domain and using wall functions.

Considering the consequences attained by the five various turbulent models, it was found that the RNG k-ε model gives exaggerated results, which are observable in Figs. 3 and 4. The Realizable k-ε model also overestimates the velocity values since both turbulent models are designed for more strongly curved flow types. Consequently, the model may be appropriate to simulate rather more swirling flows. According to Table 1, the k-ω model in conjunction with VOF

model can accurately predict the free surface evolution. However, small discrepancy was noticeable while comparing its efficiency with other turbulent models for numerical velocity values. Moreover, the RSM model following with the Standard k-ε model showed better performances in predicting flow details, such as velocity distributions, both in the regions of straight or curved flow types. Nevertheless, the RSM model involves extra equations, requires more CPU time and is computationally much more expensive. Accordingly, the Standard k-ε model can be introduced as the preferable turbulence model to deal with numerical simulations of flow in sharp open channel bends.

Nomenclature

C_1 ,C_2 C_ε, C_μ	turbulence model constants
D_{ij}	transport by diffusion (m)
E	mean rate of deformation tensor
G_b	generation of turbulence kinetic energy due to buoyancy
g	acceleration due to gravity (m/s^2)
I	turbulent intensity
L	turbulence characteristics length (m)
P	rate of production
p	pressure (N/m^2)
R_e	Reynolds number
t	time (s)
u,v	velocity components (m/s)
x,y,z	axial coordinates (m)
α	constant coefficient
β	constant power
ε	dissipation kinetic energy, m^2/s^3
τ	shear stress, N/m^2
μ	viscosity (Pa.s)
μt	turbulent viscosity
ρ	density (kg/m^3)
υ	kinematic viscosity
σ	Stefan-Boltzmann constant ($w/m^2.k^4$)
∏	transport due to turbulent pressure-strain interactions
Ω	transport due to rotation
Subscripts	
Exact	measured value
i,j	node number
ε	diffusivity
t	Turbulent

References

Akhtari, A. A. (2010). Surveying flow in strongly-curved open channel and evaluation of the effect of internal non submerged vanes on flow pattern through the bends. Civil Engineering Department. PhD Dissertation, Mashhad, Ferdowsi University of Mashhad.

Akhtari, A. A., J. Abrishami, et al. (2009). "Experimental investigation water surface characteristic in strongly-curved open channels." Journal of Applied Sciences 9(20): 3699-3706.

Blanckaert, K. and H. J. de Vriend (2003). "Nonlinear modeling of mean flow redistribution in curved open channels." Water Resources Research 39(12): 1375.

Blanckaert, K. and H. J. de Vriend (2005). "Turbulence characteristics in sharp open-channel bends." Physics of Fluids 17(5): 055102-055115.

Blanckaert, K. and W. Graf (2001). "Mean Flow and Turbulence in Open-Channel Bend." Journal of Hydraulic Engineering 127(10): 835-847.

de Vriend, H. J. (1976). A Mathematical Model of Steady Flow in Curved Open Shallow Channels, Delft University of Technology, Department of Civil Engineering, Laboratory of Fluid Mechanics.

Engelund, F. (1974). "Flow and Bed Topography in Channel Bends." Journal of the Hydraulics Division 100(11): 1631-1648.

Gaudio, P., A. Malizia, et al. (2011). "RNG k-ε modeling and mobilization experiments of loss of vacuum in small tanks for nuclear fusion safety applications." International journal of systems applications, engineering & development 1(5): 287-305.

Ghamry, H. K. (1999). Two Dimensional Vertically Averaged and Moment Equations for Shallow Free Surface Flows. Alberta, University of Alberta. PhD.

Harrington, R. A., N. Kouwen, et al. (1978). "Behaviour of a hydrodynamic finite element model." Advances in Water Resources 1(6): 331-335.

Hirt, C. W. and B. D. Nichols (1981). "Volume of fluid (VOF) method for the dynamics of free boundaries." Journal of Computational Physics 39(1): 201-225.

Hsieh, T. and J. Yang (2003). "Investigation on the suitability of two-dimensional depth-averaged models for bend-flow simulation." Journal of Hydraulic Engineering 129(8): 597-612.

Ippen, A. T. and P. A. Drinker (1962). "Boundary Shear Stresses in Curved Trapezoidal Channels." Journal of the Hydraulics Division, Vol. 88, No. 5, September/October 1962, pp. 143-180 88(5): 143-180.

Jackson, J. (1995). Osborne Reynolds: Scientist, Engineer and Pioneer. Mathematical and Physical Sciences, The Royal Society Article.

Jia, Y. and S. S. Y. Wang (1992). Computational Model Verification Test Case using Flume Data. ASCE Water Forum, Baltimore, ASCE.

Jin, Y. and P. Steffler (1993). "Predicting Flow in Curved Open Channels by Depth-Averaged Method." Journal of Hydraulic Engineering 119(1): 109-124.

Jones, W. P. and B. E. Launder (1972). "The prediction of laminarization with a two-equation model of turbulence." International Journal of Heat and Mass Transfer 15(2): 301-314.

Khosronejad, A. (2010). "CFD Application in 3D flow field modeling." Journal of Water Sciences Research 2(1): 57-63.

Khosronejad, A., C. Rennie, et al. (2007). "3D Numerical Modeling of Flow and Sediment Transport in Laboratory Channel Bends." Journal of Hydraulic Engineering 133(10): 1123-1134.

Kuipers, J., C. B. Vreugdenhil, et al. (1973). Calculations of Two-dimensional Horizontal Flow: Report on Basic Research, Delft Hydraulics.

Leonard, B. P. (1979). "A stable and accurate convective modelling procedure based on

quadratic upstream interpolation." Computer Methods in Applied Mechanics and Engineering 19(1): 59-98.

Leschziner, M. A. (1979). "Calculation of Strongly Curved Open Channel Flow." Journal of the Hydraulics Division 105(10): 1297-1314.

Leschziner, M. A. and w. Rodi (1979). "Calculation of Strongly Curved Open Channel Flow." Journal of the Hydraulics Division 105(10): 1297-1314.

Lu, J. Y., J. H. Hong, et al. (2003). "Measurement and simulation of turbulent flow in a steep open-channel with smooth boundary." Journal of the Chinese Institute of Engineers 26(2): 201-210.

Molls, T. and M. Chaudhry (1995). "Depth-Averaged Open-Channel Flow Model." Journal of Hydraulic Engineering 121(6): 453-465.

Pope, S. B. (2000). Turbulent Flows, Cambridge University Press.

Rodi, W. and I. A. f. H. Research (1993). Turbulance Models and Their Application in Hydraulics: A State-Of-The-Art Review, Balkema.

Rozovskiĭ, I. L. (1957). Flow of water in bends of open channels, Academy of Sciences of the Ukrainian SSR.

Thomson, J. (1876). "On the origin of windings of rivers in alluvial plains, with remarks on the flow of water round bends in pipes." Proceedings of the Royal Society of London 25(171-178): 5-8.

Ye, J. and J. McCorquodale (1998). "Simulation of Curved Open Channel Flows by 3D Hydrodynamic Model." Journal of Hydraulic Engineering 124(7): 687-698.